Processing and Properties of MIM AISI 4605 via Master Alloy Routes

Andrew J Coleman, Keith Murray, Martin Kearns, Toby A. Tingskog*,
Bob Sanford** & Erainy Gonzalez**

Sandvik Osprey Ltd., Red Jacket Works, Milland Road, Neath, SA11 1NJ, UK
*Sandvik Osprey Ltd., USA
** TCK S.A., Zona Franca Industrial Las Americas, Santo Domingo, Dominican Republic

ABSTRACT

AISI 4605 is one of the most popular MIM grades in use today offering good processing characteristics and relatively high strength at modest cost. For these reasons it is used in a wide variety of mechanical applications. Different raw materials combinations are used in order to achieve the final chemistry with mixtures of carbonyl iron and nickel plus elemental Mo being a typical mix option.

We report here the use of a novel 5x concentration 4605MA for manufacture of 4605 MIM parts. Parts were moulded from proprietary feedstock made using a blend of 4605MA and carbonyl iron. Tensile properties are reported for samples sintered at different temperatures and metallographic analysis was performed on as sintered and heat treated samples. It is shown that density levels of 96% are achieved and strength levels in each condition far exceed the MPIF standard levels. Results are compared with those obtained from parts made by the more conventional elemental blend route. In particular the homogeneity of parts made by each method is contrasted.

INTRODUCTION

Low alloy steel AISI 4605 is becoming more prominent in the Metal Injection Moulding (MIM) industry as the alloy of choice for a number of applications, primary in the manufacture of firearms parts but also general engineering and automotive. AISI 4605 is a hardenable nickel low alloy steel that can be used in the as sintered condition or in a higher strength heat treated condition, giving it the versatility to be used for making a wide range of components. Both nickel and molybdenum retard the transformation of high temperature austenite to ferrite plus cementite, increasing the hardenability of low alloy steels (the ease of forming martensite) and providing a fine martensite microstructure that can be tempered to develop preferred combinations of strength and toughness. There are a number ways of producing this alloys using different powder routes; 1) Carbonyl Iron Powder (CIP) + (FeNi or carbonyl Ni) + (FeMo or Mo), 2) Prealloyed (PA) powder of the desired composition, or 3) CIP + Master Alloy (MA) with either 3x or 5x concentration.

Previous work has demonstrated the benefits of using low alloy steel MAs over PA powder [1-3]. These included improved mechanical properties, better control of distortion, better control of chemistry and cost advantages. By comparison with industry standards, it was implied in previous publications that parts produced using MAs of AISI 4140 and 4340 would also have advantages over the properties of parts produced by conventional CIP + elemental powder blends: however, no direct comparisons were made. In this study we aim to demonstrate that using 4605MA can indeed give properties exceeding industry standards whilst also making a direct comparison with properties of MIM parts produced using conventional CIP + elemental powder blends. In addition, the effect of increasing sintering temperature on mechanical properties and microstructures is examined.

Published data for as sintered and heat treated MIM AISI 4605 parts are shown in Table 1. These demonstrate the wide range of mechanical properties achievable from this alloy by heat treatment.

Table 1: Published values for AISI 4605 [4-6].

4605	MPIF		BASF		German & Bose	
	AS	HT	AS	HT	AS	HT
% density					96	96
Density (g/cc)	7.5	7.5	7.55			
0.2% YS Mpa, ksi	207 30	1482 215	≥400 58	1500 218	205 30	1480 215
UTS MPA, ksi	441 64	1655 240	≥600 87	1900 276	440 64	1655 240
%El	15	2	≥5	≥2	15	2
Hardness HRC	62 HRB	48 HRC	≥150Hv10	≥55 HRC	62 HRB	48 HRC

EXPERIMENTAL PROCEDURE

Low alloy steel 4605 MA, Fe38Mo and Ni powder were produced by Sandvik Osprey's proprietary inert gas atomisation process using nitrogen gas. All gas atomised powders were air classified to a particle size distribution of 90%-22um. Carbonyl Iron Powder (CIP), containing either high or low carbon, was obtained from Sintez. For the purposes of this paper, MA+CIP refers to parts produced using MA and CIP powder whilst CIPB refers to parts produced using CIP + Fe38Mo + Ni. In all instances the mix was such that the final sintered part met the desired chemistry. The chemistry of the powder batches used is shown in Table 2.

Table 2: Chemical specification and measured analysis for powders used in this study, a) 4605 powders and b) 4605(HC)

a)

	4605MA 90%-22um			MA+CIP *90%-15um*			MA+CIP *90%-15um*		
Elem.	%wt	Min	Max	%wt	Min	Max	%wt	Min	Max
C	0.41	0.40	0.60	0.59	0.40	0.60	0.56	0.40	0.60
Ni	10.6	9.0	11.0	2.57	1.5	2.5		1.5	2.5
Mo	1.5	1.5	2.0	0.3	0.2	0.5		0.2	0.5
Si	0.54		2.0	0.108		1.0			1.0
N	0.02			0.026					
O	0.12			0.23					

b)

	4605MA 90%-22um			MA+CIP(HC) *90%-15um*			Carbonyl route CIPB(HC)		
Elem.	%wt	Min	Max	%wt	Min	Max	%wt	Min	Max
C	0.41	0.40	0.60	0.75	0.40	0.60	0.77	0.4	0.6
Ni	10.6	9.0	11.0	2.14	1.5	2.5	2.14	1.5	2.5
Mo	1.5	1.5	2.0	0.34	0.2	0.5	0.37	0.2	0.5
Si	0.54		2.0	0.14		1.0	0.009		1.0
N	0.02			0.62			0.73		
O	0.12			0.1			0.17		

For both the MA+CIP route and CIPB, feedstock was produced with carbon content meeting the carbon specification for AISI4605 of 0.4-0.6% and a second batch with a higher carbon content of ~0.75%. The higher C feedstocks were produced to determine the effect of carbon content on the mechanical properties of MIM components. For the purposes of this article the grades containing higher carbon are designated (HC).

Two grades of Sintez CIP powder were used in order to control carbon content. The high carbon grade has the following composition; 0.83% C, 0.34% O, 0.76% N and 0.0006% S. The low carbon (BC) grade has composition; 0.016% C, 0.42% O, 0.007% N and 0.0006% S. The fraction of each of these CIP powders used in each feedstock along with the powder loading, shrinkage and Melt Flow Index (MFI) values are shown in Table 3.

Feedstocks were prepared at different powder loadings using TCKs proprietary binder. 4605 MA+CIP feedstocks were prepared with 17.4% shrinkage and 20% shrinkage. For the high C variant the powder loading was reduced to 56.93% giving a shrinkage of 20.66%. The CIPB powder was prepared to the same specification. The latter shrinkage value was chosen to correspond closely to that of other commercial MIM feedstock. In the case of the CIPB(HC) powder, which has a much finer psd then this is not far from optimal powder loading based on MFI values. However, in the case of the MA+CIP(HC), powder loading was not optimised and typically shrinkage of 17.4% would be more suitable. This factor must be kept in mind when reviewing the data shown in the following sections.

To distinguish between the different shrinkage factors for the MA+CIP feedstocks an additional identifier is used in the feedstock name indicating shrinkage. For example MA+CIP17.4% designates feedstock produced using MA+CIP with a powder loading giving sintered shrinkage of 17.4%.

The feedstocks were injection moulded (Arburg) and sintered by TCK, to produce MIMA standard tensile and Charpy bar test specimens.

Table 3: CIP content and feedstock properties

	MA+CIP *90%-15um*	MA+CIP *90%-15um*	CIPB	MA+CIP(HC) *90%-15um*	Carbonyl route CIPB(HC)
5x MA	Y	Y	N	Y	N
CIP	20%BC 60%HC	20%BC 60%HC	75% HC 21.5% BC	80% HC	Y
Ni	-	-	Y	-	Y
FeMo	-	-	Y	-	Y
%C	0.59	0.59	0.56	0.75	0.77
% Loading	61.80	57.87		56.93	56.93
%Shrinkage	17.4	20.0	20.66	20.66	20.66
Melt Flow Index	86.21	189.9		156.5	203.3

Sintering

Green parts were subject to an initial solvent debind followed by a thermal debind at 500°C (932°F) and sintered in a nitrogen atmosphere. Sintering was carried out in the range 1140°C to 1360°C (2084-2480°F) with a holding time at the sintering temperature of 2 hours. Sintered parts were allowed to slow cool under a nitrogen atmosphere. As sintered tensile samples were kept for triplicate testing and

further samples were solutionized for 60mins at 830°C (1526°F), oil quenched and tempered at 200°C for 1 hour followed by air cooling. The heat treatment parameters were chosen to achieve peak hardness following initial heat treatment trials over a range of tempering temperatures.
Tensile testing was carried out on three specimens in each condition in accordance with ASTM E8-08. Vickers hardness testing was carried out using a 10kg weight. Sintered density measurements were carried out using a Micromeritics Accupyc II1340 Helium Pycnometer. Polished cross-sections of Charpy bars were prepared for porosity measurements and microstructures were analysed in the polished and etched (3% Nital) conditions.
In order to evaluate distortion during sintering, Charpy test bars were suspended across refractory supports, separated by 38mm in the sintering furnace as shown in Fig. 1a. After sintering, images of the deflection of the Charpy bars were captured and distortion measured.

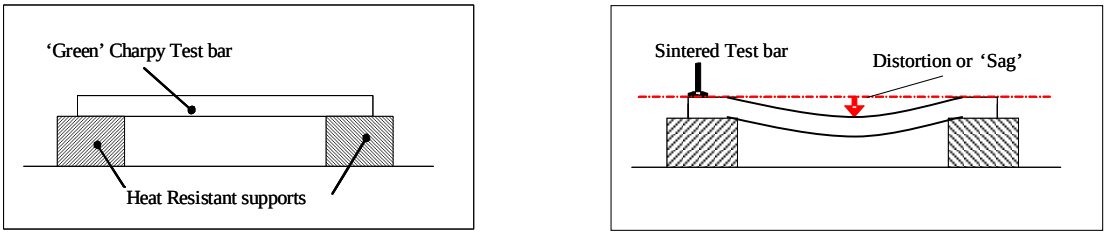

Figure 1: a), Distortion test configuration and b), example of distortion after sintering

RESULTS

As-sintered parts were analyzed for C content to confirm that the final C content fell within the target specification of 0.4-0.6% for 4605 and ~0.7% for the high C variants. Table 4 shows a summary of the C contents for each feedstock across the range of sintering temperatures used. From this it is evident that C content was well controlled for all powder variants across all sinter temperatures.

Table 4: C content as measured in as-sintered parts

	Carbon (%)					
Alloy ID	**Powder**	**1140°C**	**1200°C**	**1250°C**	**1300°C**	**1360°C**
MA17.4%	0.59	0.43	0.43	0.44	0.42	0.42
MA20%	0.59	0.44	0.44	0.44	0.44	0.42
CIPB	-	-	-	0.57	-	0.54
MA20.66%	0.75	0.69	0.7	0.71	0.67	0.67
CIPB(HC)	0.77	0.69	0.73	0.69	0.67	0.67

Densification

Pycnometric density values were measured for both the tensile bars and Charpy bars produced. There is a systematic difference in density between the two parts geometries with the thinner section tensile bars typically having 1-2% higher density than the Charpy bars. The Charpy bars have a cross-section of 10mm compared with ~3.2mm for the tensile bars and so the difference in density between the parts is attributed to this difference in thickness of the parts.
The density data for the tensile bars is shown in Figure 2~~Figure 2~~~~Figure 2~~. For all the feedstocks produced, the density increased with increasing sintering temperature and no plateau in values was observed, suggesting that full density may not have been reached. The CIPB(HC) feedstock typically reached the highest or equal highest values across the range of sintering temperatures. Given the finer psd of the starting feedstock and the impact of the higher carbon content in reducing the solidus temperature for the alloy, this is perhaps not surprising. However, the MA+CIP(HC) feedstock which had not been prepared with optimum powder loading achieved almost the same

density values as the CIP(HC) suggesting that higher values than the CIPB(HC) powder may be possible with optimum loading.

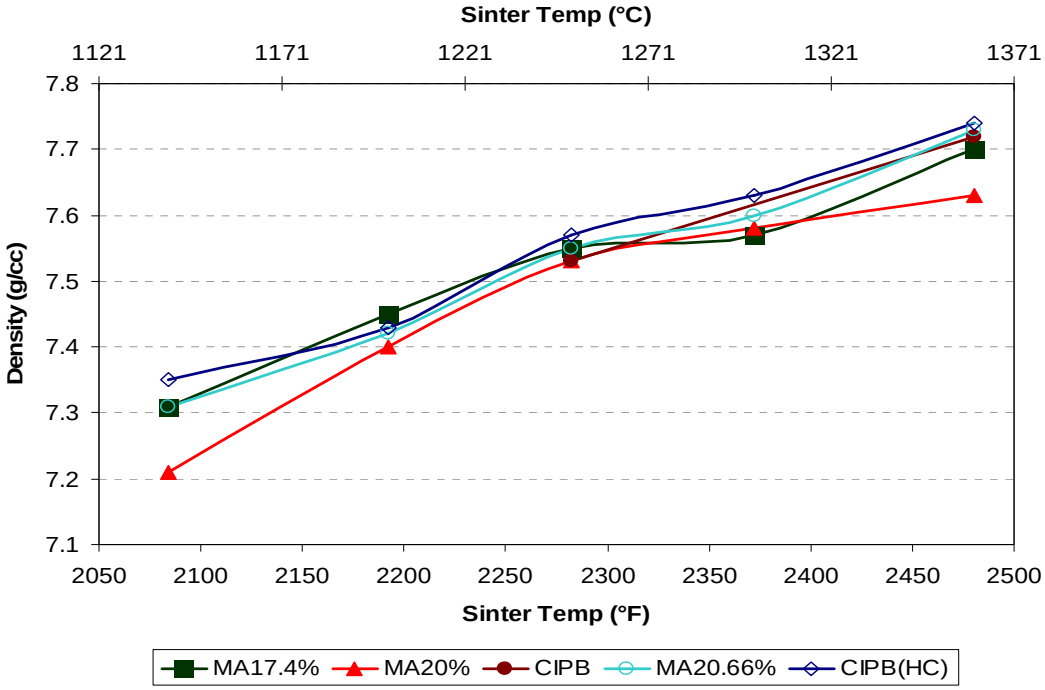

Figure 2: Pycnometric density of 4605 tensile bars (solid) and 4605(HC) tensile bars (hollow)

Of the 4605 MA+CIP feedstocks, the highest densities were observed for the MA+CIP17.4% blend. Comparable densities were obtained with MA+CIP17.4% and CIPB feedstocks.

After furnacing, cross-sections of Charpy bars were prepared for metallographic analysis of both the polished and etched surfaces. Figure 3 shows images of a) CIPB(HC) and b) MA+CIP17.4%. Both show a reduction in the number of pores with increasing sinter temperature, confirming density measurements, whilst there is also a coarsening of the pores. There are slightly fewer pores in the CIPB(HC) parts sintered at 1360 C compared with MA+CIP17.4% feedstock reflecting the higher densities obtained, as shown in Figure 2.

a)

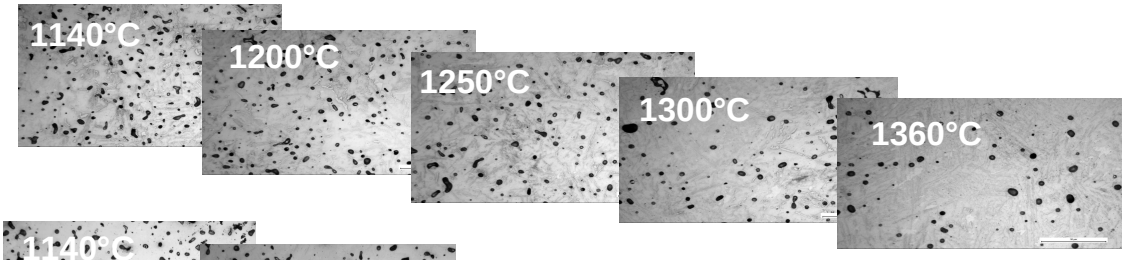

b)

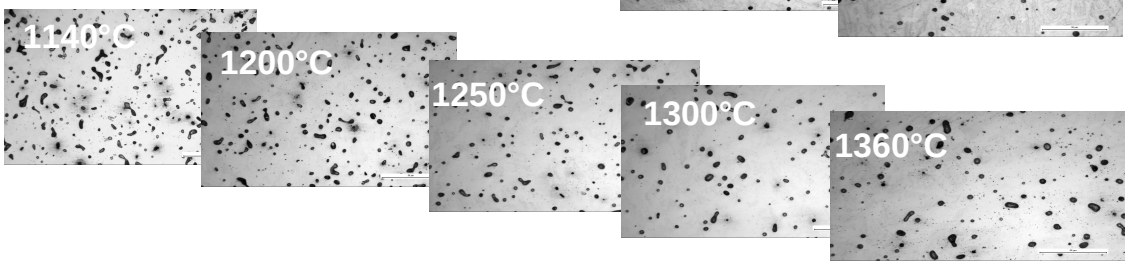

Figure 3: Micrographs of as-polished Charpy bar cross-sections of a) CIPB and b) MA+CIP17.4%.

Etched microstructures were prepared and analysed for all feedstocks. Figure 4 shows the change in as-sintered microstructure for parts produced using alloy 4605 MA+CIP17.4% as a function of sintering temperature at; a) 1140 °C, b) 1200 °C, c) 1300 °C and d) 1360 °C. At the lower sintering temperatures a light Ni-rich phase is present surrounded by bainite. As the sintering temperature increases further, transformation to bainite occurs followed by coarsening.

In the case of the CIPB(HC) feedstock shown in Figure 5 the percentage of the light, high Ni phase present is reduced across the range of sinetring temperatures. At temperatures ≥1300°C the microstructure is almost fully bainitic and although some coarsening of the bainite occurs at 1360°C, the final microstructure os not as coarse as that of the MA+CIP17.4% shown in Figure 4d..

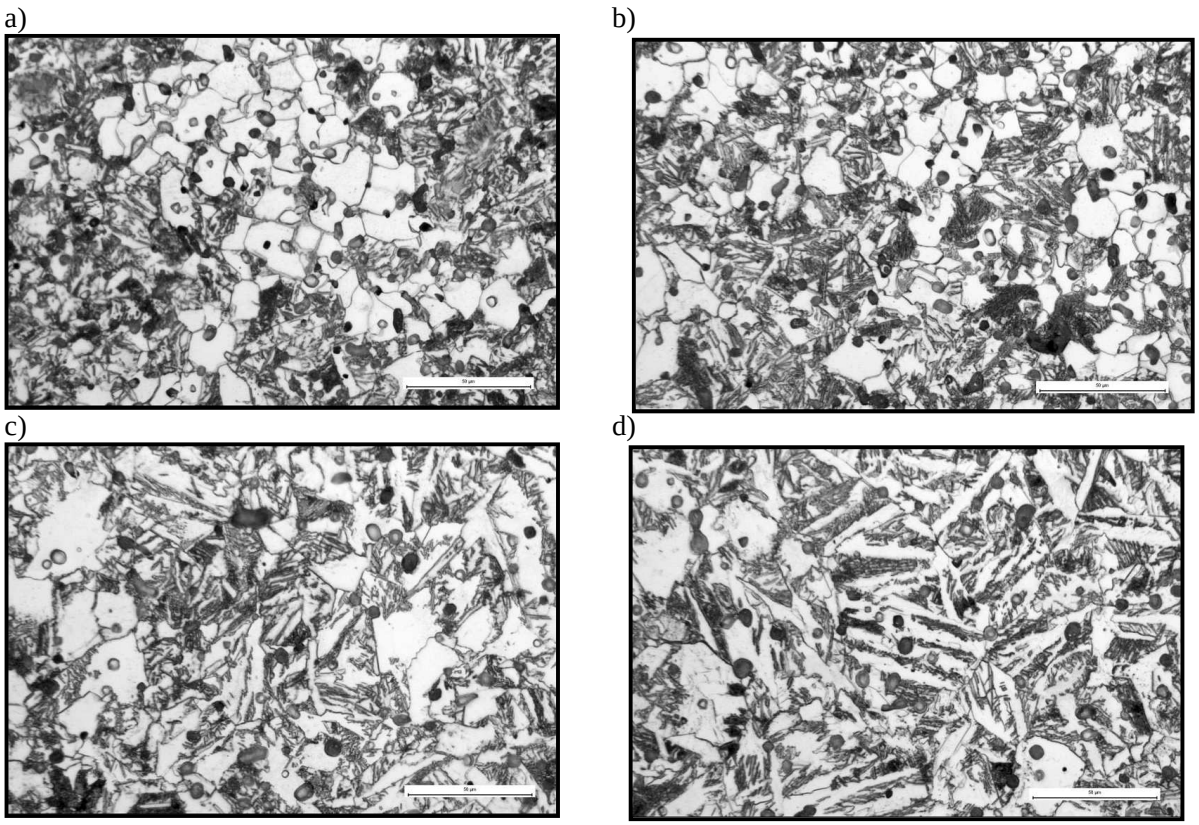

Figure 4: Shows the effect of changing sintering temperature on as-sintered microstructure of 4605MA+CIP 17.4% a) 1140°C, b) 1200°C, c) 1300°C and d) 1360°C

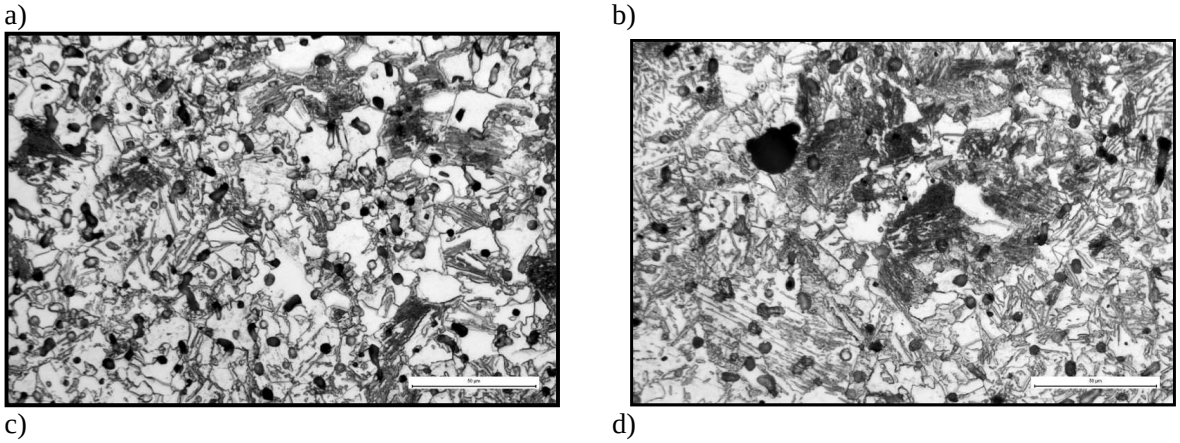

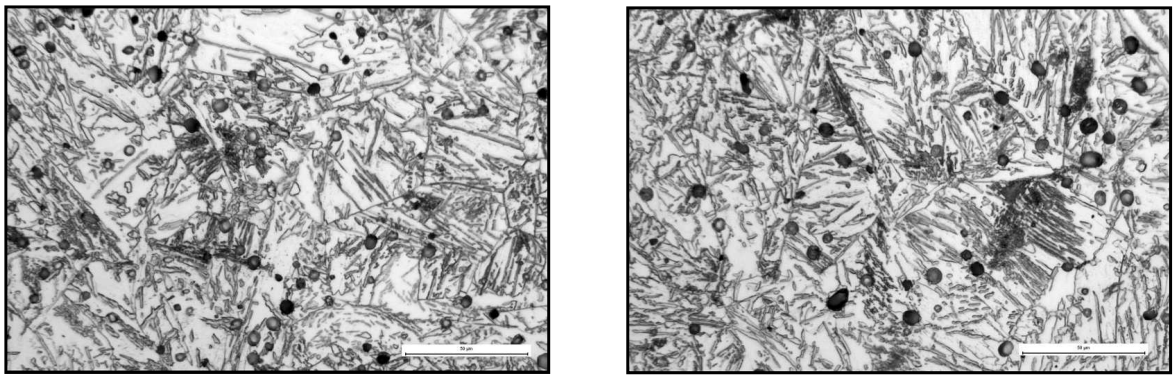

Figure 5: Shows the effect of changing sintering temperature on as-sintered microstructure of CIPB(HC) a) 1140°C, b) 1200°C, c) 1300°C and d) 1360°C

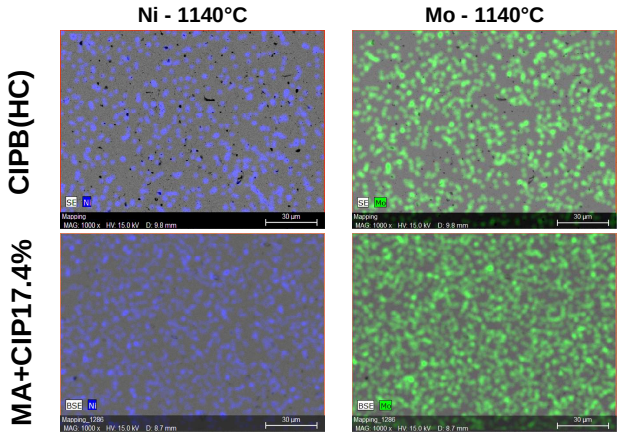

Figure 6: EDS images for CIPB(HC) and MA+CIP17.4% showing the distribution of Ni and Mo following sintering at 1140°C

EDS images were taken for sintered specimens across the range of sintering temperatures. Figure 6 shows the distribution of Ni and Mo in MIM parts produced from MA+CIP(HC) and MA+CIP17.4% following sintering at 1140°C. At this sintering temperature differences in the distribution of these elements is observed with the MA+CIP17.4% part appearing more homogeneous. As sintering temperature increased this effect became less apparent and at temperatures ≥1300°C no discernible difference was visible.

Distortion

Distortion measurements for Charpy bars as a function of sintering temperature are shown in Figure 7. Data from CIPB sinter trials were not available at the time of writing this article but images taken after sintering showed similar distortion results to the CIPB(HC) Charpy bars.

In most instances the lowest distortion was observed at 1140°C. However, at this temperature full densification had not occurred. At higher sintering temperatures lowest distortion was typically observed at 1300°C. At temperatures above this the distortion increased.

The MA+CIP variants prepared with higher shrinkage factors of 20% and 20.66% (powder loadings of 57.87% and 56.93% respectively) exhibited higher distortion than the MA+CIP17.4% feedstock with a powder loading of 61.8%. Distortion results for the CIPB(HC) and MA+CIP17.4% feedstocks were comparable across the range of sinter temperatures.

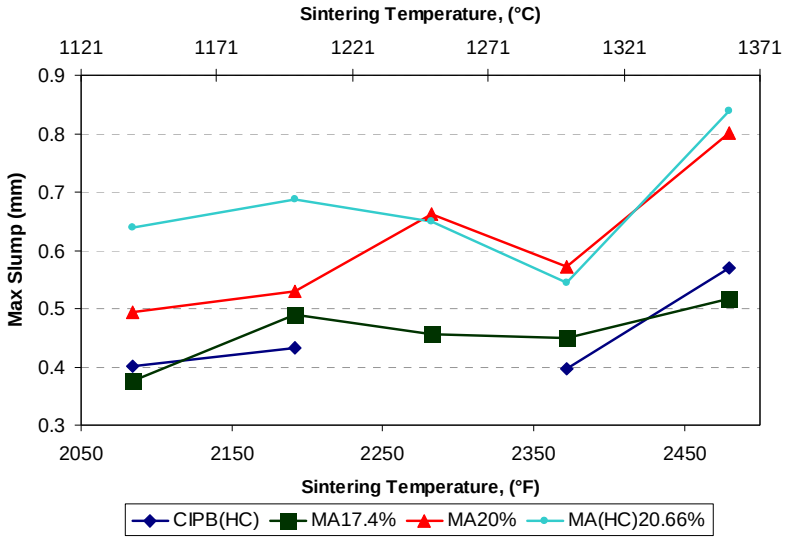

Figure 7: Distortion as a function of sintering temperature

Mechanical Properties

Tensile tests were carried out in both the as-sintered and heat treated states. Proof stress results are shown in Figure 8 for; a) as sintered and b) heat treated parts. Hollow symbols indicate the high carbon variants whilst the solid symbols are for the 4605 MA+CIP and CIPB feedstocks. Focusing on the 4605 MA+CIP and CIPB feedstocks initially, it is clear that in the as-sintered condition the MA+CIP feedstocks achieved higher proof stress values than the CIPB feedstock. Comparing with values reported elsewhere (shown in Table 1) then properties obtained for both the MA+CIP and CIPB feedstock used in this study exceed the minimum MPIF standard. However, only the MA+CIP feedstocks sintered at temperatures ≥1300C achieved the minimum value of 400MPa reported by BASF [5].

For higher carbon feedstocks the MA+CIP(HC) feedstock exhibited values 30-60MPa higher than the CIPB(HC) feedstock across the range of sinter temperatures used in this study. The MA+CIP(HC) feedstock also exhibited values from 60 to 120MPa higher than the MA+CIP17.4% feedstock.

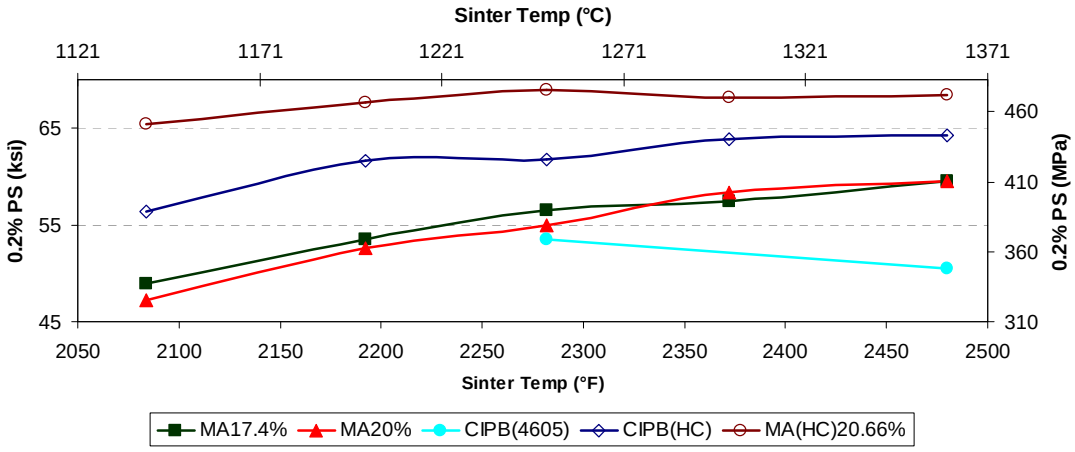

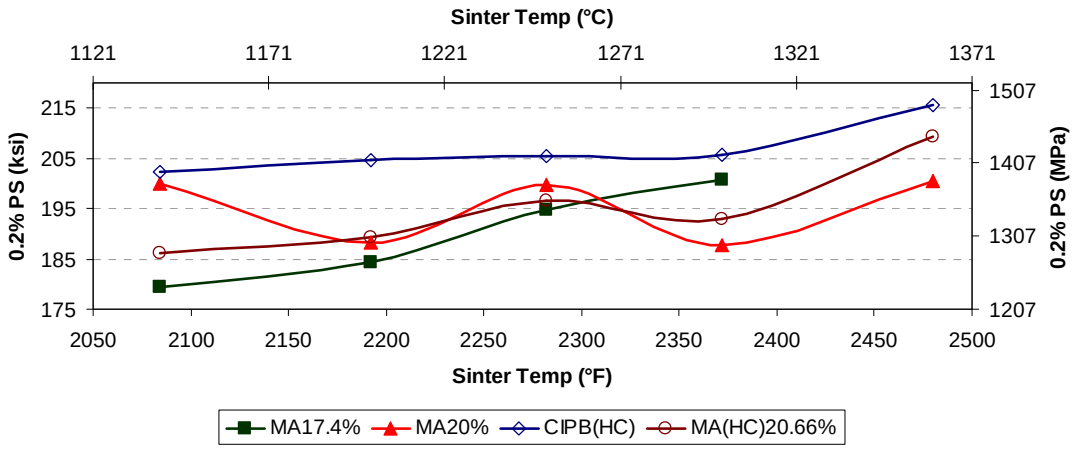

Figure 8: 0.2% Proof Stress values for (a) as sintered and (b) heat treated MIM tensile bars. Solid symbols denote 4605 feedstocks and hollow symbols the HC grades.

Figure 8b shows the proof stress values for parts in the heat treated condition. At the time of writing data was not available for heat treated bars of CIPB. Focusing on the high carbon grades initially, then it is evident that there has been a reversal in the trends observed for the as-sintered parts, with the CIPB(HC) feedstock now exhibiting higher proof stress values than the MA+CIP(HC) feedstock across all sinter temperatures.

In the case of the 4605 feedstocks values up to 1385MPa were observed at 1300C for the MA+CIP17.4% feedstock. However, values reported elsewhere and shown in Table 1 for 4605 MIM parts in the heat treated condition demonstrate that values up to 1500MPa are possible. Although initial trials were carried out to try and optimise the heat treatment used in this study, further work is required to improve heat treatment properties. It is also evident that the heat treatment used has a bigger impact on the properties of the CIPB(HC) than the equivalent MA+CIP feedstock. The reasons for this are not fully understood and further work is required.

DISCUSSION

The alloy chosen is this study, AISI 4605, is a popular low alloy steel currently used within the MIM sector and today a CIP+elemental powder blend recipe is most commonly used for the production of MIM feedstock.

As sintered properties of MIM parts produced using CIPB feedstock in this study are comparable with industry standards shown in Table 1 and provide a good reference for making comparisons with the mechanical properties for parts produced using MA+CIP. Differences in properties between the CIPB parts produced in this study and other data may be linked to the elemental powder that is used. In this study 90%-22um gas atomised Ni and Fe38Mo powder was used. However, other commercial formulations may feature fine carbonyl nickel and elemental Mo powder. The choice of starting ingredients can affect diffusion and sintering processes which in turn may influence properties.

Due to the high proportion of very fine CIP powder used in this feedstock, the interparticle spacing is smaller than the MA+CIP feedstocks and this is reflected in the higher melt viscosity shown in Table 3. Despite this the MA+CIP(17.4%) showed comparable distortion results and actually exhibited lower distortion at the highest sintering temperature, 1360C. Reducing the powder loading so that shrinkage on sintering was 20% caused an increase in the distortion on sintering. This and the higher densities observed for the MA+CIP17.4% feedstock indicate that this is the optimum powder loading for the MA+CIP powder.

Tensile properties for the MA+CIP 4605 feedstocks were equal to or higher than those parts produced using CIPB and meet or exceed industry minimum standards. Previous work by the authors has demonstrated that for low alloy steels 4140 and 4340 MIM parts produced using MAs have higher mechanical properties than those produced using pre-alloyed powder. It was hypothesised in those reports that MAs could also produce MIM parts with higher mechanical properties than CIP+elemental powder due to the problems associated with obtaining a fully homogeneous microstructure using this route. EDS measurements in this study show that at sintering temperatures <1300°C the distribution of alloying elements Ni and Mo is more homogeneous in the MA formulation although at temperatures ≥1300°C the distribution of elements is similar. The mechanical properties reported do demonstrate however, that the MA route can still produce MIM parts with higher mechanical properties than CIP+elemental powders.

As would be expected, increasing carbon content increased the tensile strength. Interestingly the effect was more pronounced on parts produced using MA than those produced using CIP+elemental powder, increasing proof stress by 60-120Mpa. This resulted in the MA parts having proof stress values 30-60MPa higher than the CIPB(HC) across the range of sinter temperatures.

Properties of heat treated samples showed a reversal in the trend observed for the high carbon as-sintered parts. However, the mechanical properties obtained for the CIPB(HC) feedstock still did not exceed those reported elsewhere (shown in Table 1). Based on this result it can be concluded that the heat treatment cycle used in this study was not fully optimised and further work is required in this area for a full comparison to be made.

SUMMARY & CONCLUSIONS

A novel 5 x concentration 4605 MA has been produced. Combined with CIP it can be sintered to give as sintered tensile properties equal to or higher than the industry standard CIP+elemental powder route. Good control of carbon was achieved over the range of sintering temperatures evaluated and final density ranged from 96-99% theoretical depending on sintering temperature. Tensile bars typically exhibit 1-2% higher final density than Charpy bars.

The feedstock with lowest powder loading and highest carbon level gives highest property levels: superior to ‘CIP-only’ material with same C level. Above 2300F, all feedstocks give %El higher than as sintered book values. Heat treated properties show an improving trend with sintering temperature and the ‘CIP-only’ variant (with high C) gives highest proof strengths. Tempering conditions need to be optimised for MA + CIP variants to match the ‘CIP-only’ material.

When powder loading is optimised for 4605 MA+CIP feedstock, distortion during sintering can be controlled to match that of parts produced using CIP+elemental powder. Distortion is evident at >2400^{o}F for all samples.

As sintering temperature increases, grains coarsen and diffusion leads to a change in microstructure from ferrite plus pearlite to homogeneous, coarse-lath bainite. EDAX analysis shows that the MA route gives more uniform distributions of Ni, Mo in low temperature sintered materials but this difference is not apparent at higher temperatures.

ACKNOWLEDGEMENTS

Thanks are due to Ms. Linn Larsson of Sandvik Materials Technology, Sandviken, for coordinating metallographic studies.

REFERENCES

1. T.A. Tingskog, G.J. Del Corso, M.L. Schmidt and D.T. Whychell, " Diffusion of Alloying Elements During Sintering of MIM Master Alloys", Advances in Powder Metallurgy & Particulate Materials – 2002. Proceedings of the 2002 International Conference on Powder Metallurgy & Particulate Materials, Part 10, 156
2. P.A. Davies, G.R. Dunstan, D.F. Heaney and T.J. Mueller, "Comparison of Master Alloy and Pre-Alloyed 316L Stainless Steel Powders For Metal Injection Molding (MIM)", PM2TEC 2004 World Congress, MPIF, Chicago, IL.
3. A.J. Coleman, K. Murray, M.A. Kearns, T. A. Tingskog, B. Sanford, E. Gonzalez, "Effect of Particle Size Distribution on Processing and Properties of Metal Injection Moulded 4140 and 4340", PowderMet 2011, San Francisco, CA
4. Metal Injection Moulding: A Manufacturing Process for Precision Engineering Components, EPMA
5. Catamold ® 4605 Data Sheet, 2006, BASF
6. Injection Molding of Metals & Ceramics, R M German & A Bose MPIF, 1997